Available online at www.sciencedirect.com
ScienceDirect
Journal of Nutritional Biochemistry 18 (2007) 322–331
Journal of Nutritional Biochemistry

Regulation of adipocyte differentiation by PEGylated all-*trans* retinoic acid: reduced cytotoxicity and attenuated lipid accumulation

H.S. Moon[a], D.D. Guo[a], H.H. Song[a], I.Y. Kim[a], H.L. Jin[a], Y.K. Kim[a], C.S. Chung[b], Y.J. Choi[a], H.K. Lee[a], C.S. Cho[a,*]

[a]*School of Agricultural Biotechnology, Seoul National University, Seoul 151-742, South Korea*
[b]*College of Agriculture, Life and Environment Sciences, Chungbuk National University, Cheongju 361-763, South Korea*

Received 24 March 2006; received in revised form 19 June 2006; accepted 27 June 2006

Abstract

Obesity is major risk factor for many disorders, including diabetes, hypertension and heart disease. Unfortunately, there is a dearth of therapeutic agents available to clinicians for the treatment of obesity. The principal aim of this study was to investigate whether PEGylated all-*trans* retinoic acid (PRA) can have favorable stability and biological activity in 3T3-L1 preadipocytes as an antiobesity drug. Here, we found that PRA inhibits the process of adipogenesis, including survival of adipocytes and differentiation to mature adipocytes. The results showed that RA nanoparticles (NPs) were prepared by PEGylation; below 200 nm, PRA-NPs were obtained. Moreover, PRA decreased glycerol-3-phosphate dehydrogenase activity in 3T3-L1 preadipocytes by acting with major adipocyte marker proteins such as PPARγ2, C/EBPα and aP2 modulators. Apoptosis, in addition, increased as the level of RA increased from 10 to 20 μM, whereas PRA reduced apoptosis with increasing concentrations. Our data suggest that PRA-NP has potential as an antiobesity drug carrier due to its small particle size and PEGylated core–shell structure. In addition, our results suggest that PRA inhibits the process of adipogenesis and may be developed to treat obesity. Based on these results, PRA is suitable for adipocyte studies, and an enhanced effect of PRA with adipocyte differentiation offers a challenging approach for pharmaceutical applications.

Keywords: Poly(ethylene glycol) (PEG); All-*trans* retinoic acid (RA); Adipocyte differentiation; PEGylation; Antiobesity

1. Introduction

Advances in adipose tissue biology over the past 10 years have led to an improved understanding of the mechanisms linking obesity with metabolic syndrome and other complications. Adipocytes play a central role in maintaining lipid homeostasis and energy balance in vertebrates by storing triacylglycerides (TGs) or by releasing free fatty acids in response to changes in energy demands [1,2]. However, obesity is associated with a number of pathological disorders such as non-insulin (INS)-dependent diabetes, hypertension, hyperlipidemia and cardiovascular diseases [3]. Several lines of evidence have suggested that TG accumulation in skeletal muscles and pancreatic islets is causally related to skeletal muscle INS resistance and pancreatic β-cell dysfunction in obese patients [4–6]. Obesity, in addition, is caused not only by adipose tissue hypertrophy but also by adipose tissue hyperplasia, which triggers the transformation of preadipocytes into adipocytes [7]. However, the molecular basis for these associations remains to be elucidated, thus rendering the search for antiobesity agents inherently difficult.

Retinoic acid regulates cellular functions by binding to intracellular retinoic acid receptors (RARs) or retinoid X receptors (RXRs). These two retinoid receptor families act via the formation of either an RAR–RXR heterodimer or an RXR–RXR homodimer, both of which regulate the expression of retinoic acid target genes [8]. Specifically, clinical trials have shown that all-*trans* retinoic acid (RA), the most active form of vitamin A metabolites, is effective against

Abbreviations: RA, all-*trans* retinoic acid; APEG, amine-terminated poly(ethylene glycol); NP, nanoparticle; PRA, PEGylated RA; ORO, Oil Red-O; NADH, β-nicotinamide adenine dinucleotide; DHAP, dihydroxyacetone phosphate; INS, insulin; Dex, dexamethasone; IBMX, 3-isobutyl-1-methylxanthine; DCC, 1,3-dicyclohexylcarbodiimide; NHS, *N*-hydroxysuccinimide.

* Corresponding author. Tel.: +82 2 880 4636; fax: +82 2 875 2494.
E-mail address: chocs@plaza.snu.ac.kr (C.S. Cho).

0955-2863/$ – see front matter © 2007 Elsevier Inc. All rights reserved.
doi:10.1016/j.jnutbio.2006.06.004

several human malignancies [9], as well as for the treatment of epithelial and hematologic malignancies such as breast [10], lung [11] and neck cancers [12]. Moreover, RA plays essential roles in the regulation of the adipogenesis of preadipocyte cell lines [13] and human osteoblasts [14,15]. However, in spite of these pronounced effects, vitamin A deficiency causes cessation of growth and night blindness, and renders organisms more susceptible to infection [16,17]. Furthermore, a high concentration of vitamin A intake results in hypervitaminosis and nausea, with severe detrimental effects [18]. In addition, the high concentration of RA induces apoptosis in adipocytes [19]. For these reasons, adipocyte differentiation studies with RA are difficult, and clinical applications of RA are also limited.

Polymers play increasingly important roles in drug formulation and drug delivery. In particular, poly(ethylene glycol) (PEG) has found a wide application in the preparation of statically stabilized liposomes, which show reduced uptake by macrophages, increase solubility in water and reduce secondary aggregation [20–22]. In fact, the Food and Drug Administration has approved the use of PEG for human intravenous, oral and dermal applications [23]. PEG is a unique polyether diol, which is generally manufactured through the aqueous anionic polymerization of ethylene oxide, although other polymerization initiators can also be employed [24]. Moreover, PEG is amphiphilic and is dissolved in organic solvents as well as in water. It is also nontoxic and can be eliminated through a combination

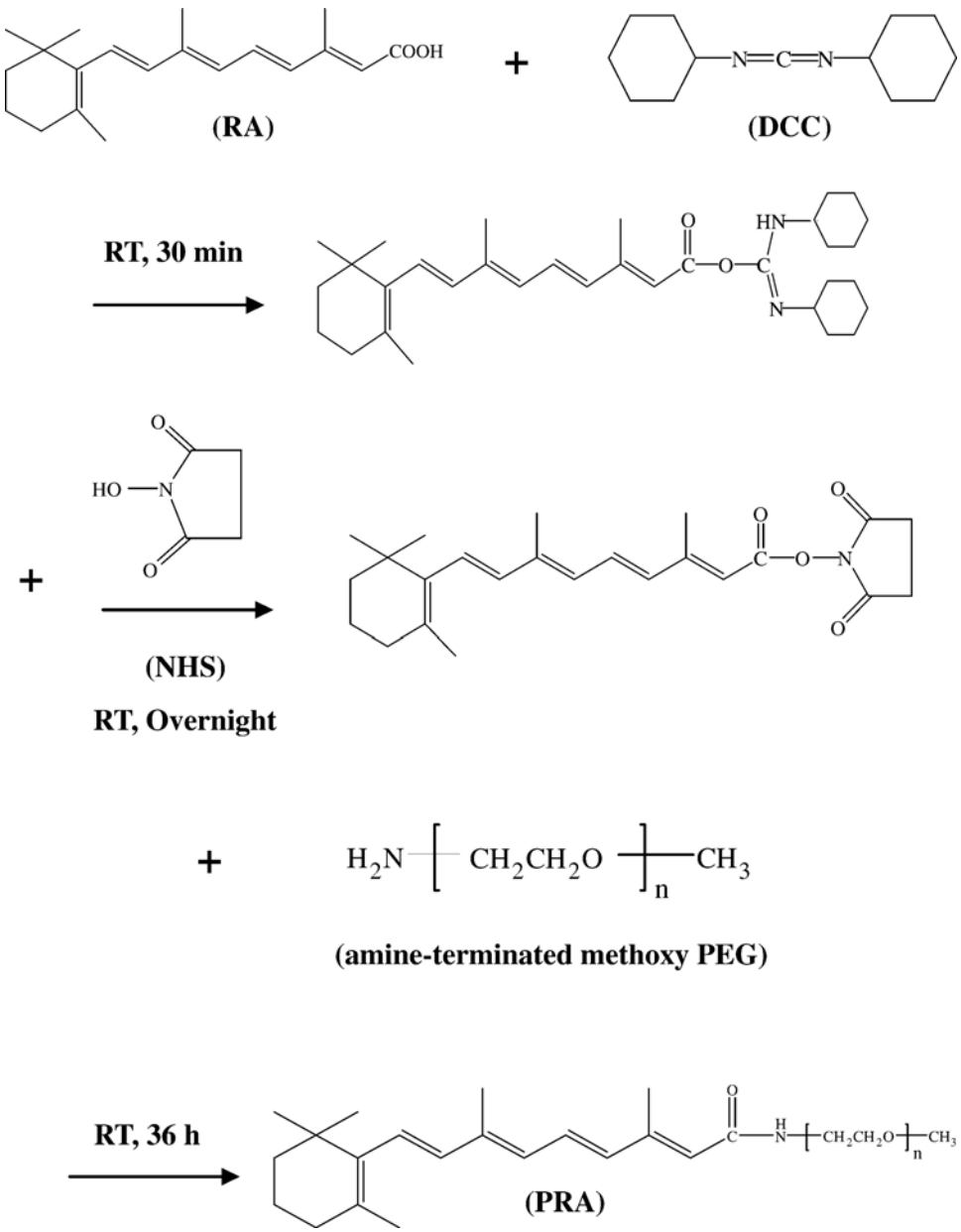

Fig. 1. The reaction scheme of PRA.

of renal and hepatic pathways, thus making it ideal for pharmaceutical applications [25].

The objective of our study was to make use of PEGylated all-*trans* retinoic acid (PRA), which has the potential for decreasing cytotoxicity and for attenuating lipid accumulation in 3T3-L1 preadipocytes for clinical applications. Attempt was also made to better understand the molecular mechanisms by which PRA affects the expression of transcription factors, differentiation and lipolysis in adipocytes.

2. Materials and methods

2.1. Materials

RA, Oil Red-O (ORO), isopropyl alcohol, β-nicotinamide adenine dinucleotide (NADH), dihydroxyacetone phosphate (DHAP), INS, dexamethasone (Dex), 3-isobutyl-1-methylxanthine (IBMX) and Dulbecco's modified Eagle's medium (DMEM) were obtained from Sigma (St. Louis, USA). 1,3-Dicyclohexylcarbodiimide (DCC) and *N*-hydroxysuccinimide (NHS) were obtained from Aldrich (Milwaukee, USA). Fetal bovine serum (FBS) and amine-terminated poly(ethylene glycol) (APEG) were purchased from Gibco Life Technologies (New York, USA) and Sunbio (Seoul, Korea), respectively.

2.2. Cell culture and differentiation induction

3T3-L1 preadipocytes were obtained from the American Type Culture Collection. Cells were seeded in 6-, 12- and 24-well tissue culture plates and grown to confluence in DMEM with 100 U/ml penicillin, 100 μg/ml streptomycin, 1 mM sodium pyruvate and 10% FBS. For standard adipocyte differentiation, 3 days after the cells had reached confluency (hereafter referred to as Day 0), the cells were exposed to the differentiation medium containing 10% FBS, 10 μg/ml INS, 1 μM Dex and 0.5 μM IBMX for 3 days and maintained in a postinduction medium containing 10% FBS and 10 μg/ml INS. Cells were grown at 37°C in 5% CO_2 incubator, and fresh medium was changed every 3 days.

2.3. Preparation of PRA

RA (108 mg, 3.6×10^{-4} mol) dissolved in 10 ml of DMSO was activated with NHS (83 mg, 7.2×10^{-4} mol) and DCC (371 mg, 1.8×10^{-3} mol) and subsequently reacted with APEG (M_W=5000) (600 mg, 1.2×10^{-3} mol) at room temperature for 36 h. The resulting solution was then dialyzed at 4°C in a dark room and freeze-dried. The reaction scheme of PRA is shown in Fig. 1. The degree of PRA was estimated by ^{1}H NMR (Avance 500; Bruker).

2.4. Transmission electron microscopy (TEM) observation

The morphology of core–shell type PRA nanoparticles (NPs) was observed using TEM (JEM 1010; JEOL, Japan). A drop of the suspension of PRA-NP in distilled water was placed on a copper grid and stained with 2% uranyl acetate solution for 20 s. The grid was allowed to dry further for 15 min prior to examination with an electron microscope.

2.5. Size distribution measurement

PRA size in aqueous solution was measured by dynamic light scattering (DLS) at a 90°C angle to the incident beam.

2.6. Stability test of PRA in light

RA and PRA were dissolved in methanol (0.01 wt.%). Samples were placed at room temperature under a 60-W light source at a 50-cm distance from the samples. At specific time intervals, changes in absorbance were determined through UV absorbance spectroscopy at 350 nm (2120UV; OPTIZEN, Seoul, Korea).

2.7. Flow cytometric analysis of cell cycle and apoptosis

3T3-L1 preadipocytes in the presence or absence of RA and PRA were collected by centrifugation and fixed with 70% ethanol at 4°C overnight. Seventy percent ethanol was then removed by centrifugation, and the DNA of the cells were stained with a propidium iodide (PI) (Sigma) staining solution [100 μg/ml PI, 0.1% Triton-X and 1 mM EDTA in phosphate-buffered saline (PBS)] in the presence of an equal volume of DNase-free RNase (200 μg/ml) (Intron Biotech., Seoul, South Korea) for 90 min and analyzed by fluorescence-activated cell sorter (FACS) analysis.

2.8. Single-color indirect DNA staining

To fix 3T3-L1 cells, 1 ml of 3.7% formaldehyde in PBS (pH 7.4) was added into plates for 20 min and washed thrice with PBS. DAPI in 1 ml of sterile dH_2O was then inserted into the plate well for 90 min and visualized.

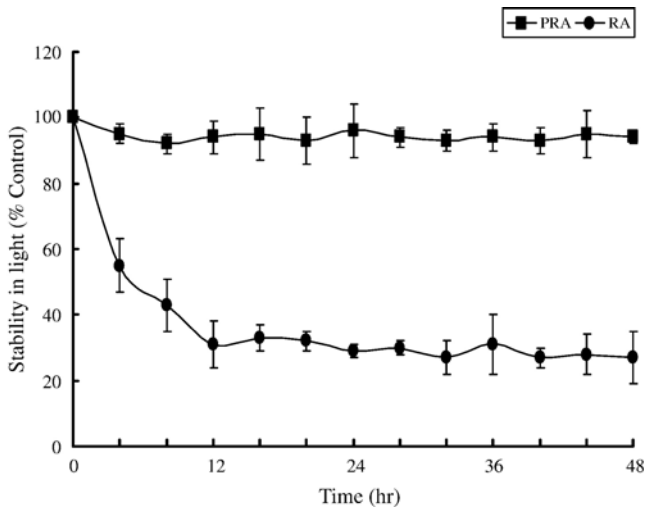

Fig. 2. Stability test of RA and PRA. At specific time intervals, changes in absorbance were determined through UV absorbance spectroscopy at 350 nm. The concentration of intact RA in the methanol solution rapidly decreased compared to that of PRA during incubation at room temperature under light exposure. Each experiment was performed in triplicate. Values are expressed as mean±S.D.

2.9. Glycerol-3-phosphate dehydrogenase (GPDH) activity

GPDH assay was performed using a spectrophotometric method to detect the disappearance of NADH during the GPDH-catalyzed reduction of DHAP under zero-order condition, as modified by Wise and Green [26]. Proteins were measured according to the Bradford method [27].

2.10. Cell viability assay

Cell viability was measured using the MTT proliferation kit (Sigma), as described by the supplier.

2.11. Lipid staining

Cells were stained with ORO, as described by Suryawan and Hu [28]. Briefly, dishes were washed thrice with PBS and fixed with 10% formalin for 1 h at room temperature. After fixation, the cells were washed once with PBS and stained with a filtered ORO stock solution (0.5 g of ORO in 100 ml of isopropyl alcohol) for 30 min at room temperature. Subsequently, the cells were washed twice with water for 15 min and visualized.

2.12. Triglyceride (TG) content

TG content was measured with a colorimetric assay that quantifies the glycerol content of the samples (GPO-Trinder; Sigma). This assay involves the enzymatic hydrolysis of TG by lipase into free fatty acids and glycerol. The glycerol moiety, through a series of oxidation–reduction reactions, then associates with 3,5-dichloro-2-hydroxybenzene sulfonate and 4-aminoantipyrine to produce a red dye. The absorbance of this dye is proportional to the concentration of TG present in each sample. Following these reactions, an aliquot of each sample was transferred into 96-well plates, and absorbance was quantified on a microtiter plate reader at 520 nm.

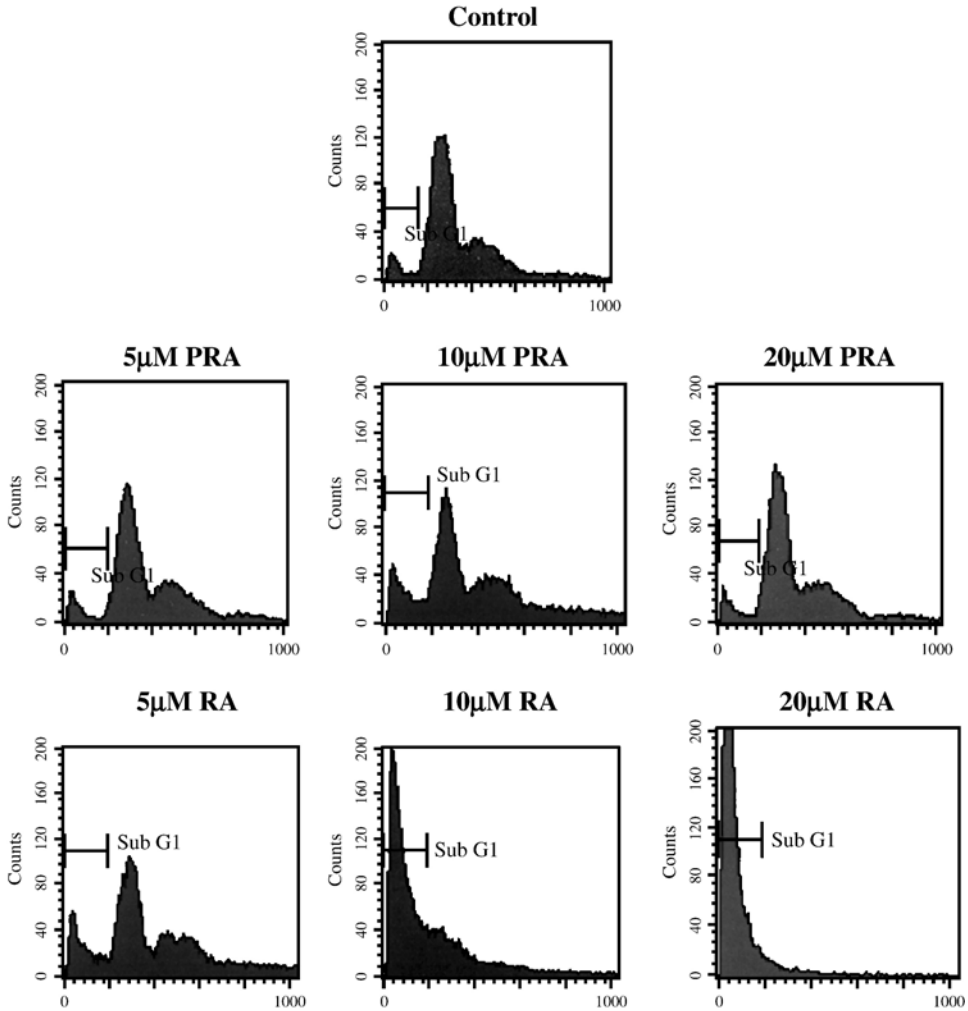

Fig. 3. Apoptosis analysis of RA and PRA in preinduction (Days −3 to 0) 3T3-L1 cells. 3T3-L1 preadipocytes were seeded in 24-well polystyrene surface (PS) plates at a density of 3×10^5 cells/well containing DMEM and 10% FBS, and treated with 0–20 μM RA and PRA for 72 h. 3T3-L1 cells were harvested and analyzed by FACS. The sub-G_1 region represents cells undergoing apoptosis-associated DNA degradation. Apoptosis was induced by 10–20 μM RA treatment in preinduction 3T3-L1 preadipocytes, whereas PRA reduced apoptosis with increasing concentrations.

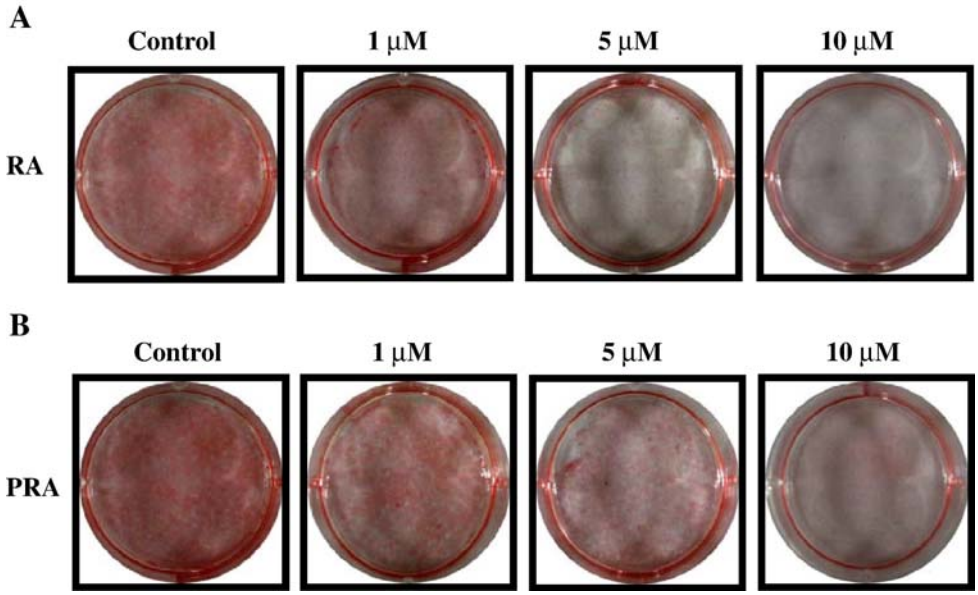

Fig. 4. Effect of 0–10 μM RA and PRA on the morphology of cultured postinduction (Days 0–15) 3T3-L1 cells. Differentiation of 3T3-L1 cells was induced following standard protocols. Cells were fixed and stained with ORO to visualize lipid content on Day 15 of differentiation. 3T3-L1 cells placed on cocktails, such as INS, Dex and IBMX, undergo full maturation into adipocytes, whereas adipocyte treatments of 1–10 μM RA and PRA blocked the accumulation of lipid droplets in the cytoplasm. (A) Postinduction 3T3-L1 preadipocytes were treated with cocktail for 15 days in the presence of 0–10 μM RA. (B) Postinduction 3T3-L1 preadipocytes were treated with cocktail for 15 days in the presence of 0–10 μM PRA.

2.13. 5-Bromo-2′ -deoxyuridine (BrdU) incorporation

After the indicated period of RA and PRA treatment, the cells were rinsed twice with PBS, and incorporation of BrdU was assayed after 2 h of incubation, according to the manufacturer's instruction (Boehringer Mannheim, Germany).

2.14. Whole cell extracts

Plates were washed twice in PBS, and the cells were lysed on the plates by adding a sodium dodecyl sulfate (SDS) sample buffer containing 2.5% SDS, 10% glycerol, 50 mM Tris–HCl (pH 6.8), 10 mM dithioerythritol, 10 mM β-glycerophosphate, 10 mM NaF, 1 mM sodium orthovanadate, 1 mM phenylmethylsulfonyl fluoride and the complete protease inhibitor mixture (1/50 tablet/ml) (Boehringer Mannheim). Cell lysis was immediately followed by 10 min of boiling, and lysates were subsequently treated with benzon nuclease (Boehringer Mannheim). Whole cell extracts were stored at −80°C. Protein concentrations were determined by the Bradford method.

2.15. Western blot analysis

Fifty micrograms of proteins was loaded onto each lane. After SDS polyacrylamide gel electrophoresis, proteins were blotted onto nitrocellulose membranes (Amersham Pharmacia Biotech., England, UK), which were then blocked overnight in TBS containing 5% nonfat dry milk and 0.1% Tween 20 (Biosesang, Seoul, South Korea). Incubation with primary and secondary antibodies was performed for 2 h in TBS containing 5% nonfat dry milk. After incubation with antibodies, the membranes were washed in TBS containing 0.1% Tween 20. The primary antibodies used were goat polyclonal adipocyte lipid-binding protein (aP2) and mouse monoclonal PPARγ, recognizing both PPARγ isoforms and mouse monoclonal antibodies against mouse C/EBPα. Secondary antibodies consisted of horseradish-peroxidase-conjugated antimouse and antigoat antibodies (Santa Cruz Biotech., USA). Enhanced chemiluminescence (Intron Biotech.) was used for detection.

2.16. Statistical analysis

Statistical analysis was performed using Student's *t* test. Data were expressed as mean±S.D. Statistical significance was represented by $*P < .05$ and $**P < .01$.

3. Results

3.1. Synthesis and characterization of PRA

Fig. 1 depicts the structures of RA, PEG and synthesized PRA. Confirmation of the synthesized PRA was performed using ^{1}H NMR (data not shown). The composition of RA in PRA, as estimated by ^{1}H NMR, was 60 mol%. It is expected that PRA, composed of PEG as the hydrophilic part and RA as the hydrophobic part, will self-assemble to polymeric NPs. As a matter of fact, the morphology of prepared PRA-NPs observed by TEM showed a spherical shape (data not shown). In addition, the size and size distribution of PRA-NPs by DLS measurement indicated that the sizes of PRA-NPs were around 200 nm, with narrow size distribution (data not shown). It has been already reported that polymeric NPs have several advantages over conventional drug carriers, including small particle size, ease of administration, drug targeting to specific body sites, increased

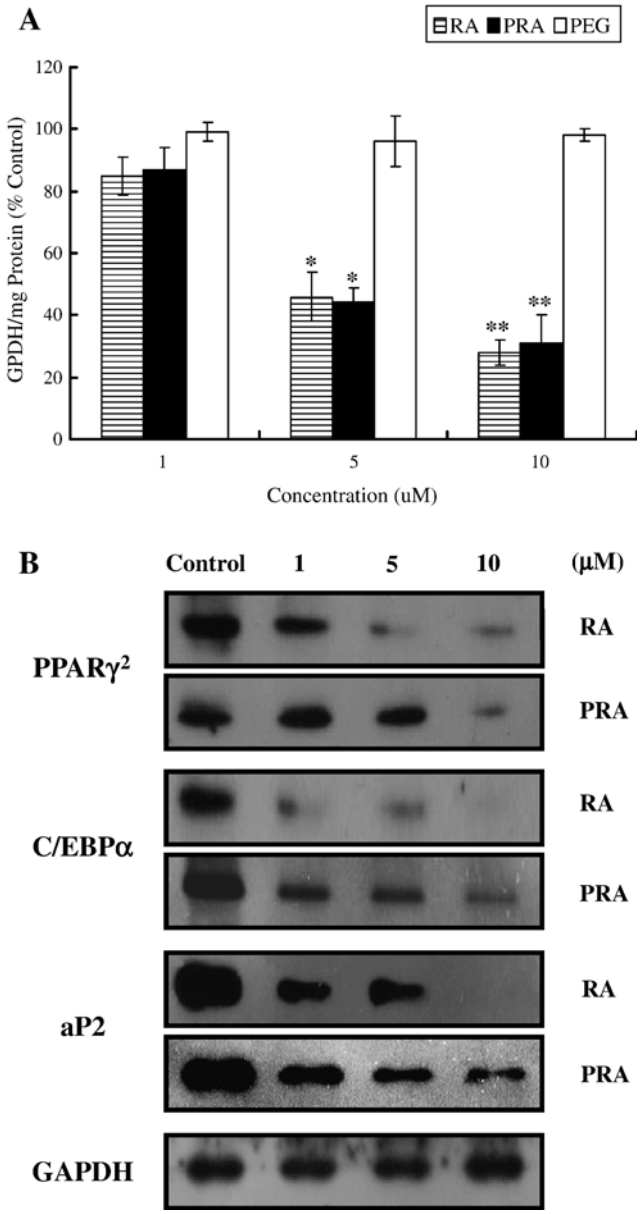

Fig. 5. Effect of 0–10 μM RA and PRA on the GPDH activity (A) and Western blot analysis (B) of postinduction (Days 0–15) 3T3-L1 cells. Adipogenesis was induced by treatment with the cocktail of 3T3-L1 preadipocytes. Subsequently, the cells were treated with RA and PRA at indicated concentrations for 15 days. (A) Postinduction 3T3-L1 preadipocytes were treated with cocktail for 15 days in the presence of 0–10 μM RA and PRA. Values are expressed as mean±S.D. *$P<.05$. **$P<.01$. (B) RA and PRA promoted the dedifferentiation of 3T3-L1 preadipocytes. Western bolt analysis showed that treatment with 1–10 μM RA and PRA inhibited the expression of major adipocyte marker proteins, which normally increase during adipocyte differentiation (nontreated cells included for comparison). Each experiment was performed in triplicate.

circulation time in the blood and solubilization of hydrophobic drugs [29–31]. Our data, together with these results, suggest that PRA-NPs have potential as an antiobesity drug due to their small particle size. Fig. 2 shows the stabilities of RA and PRA exposed to light. The concentration of intact RA in a methanol solution rapidly decreased during incubation at room temperature under light exposure. Within 8 h, less than 50% of intact RA remained in the solution, whereas the rate of PRA degradation was very slow; after 48 h of incubation, more than 90% of PRA was found intact — an indication of the increased stability of RA under light exposure by PEGylation.

3.2. Apoptosis and cell cycle analysis of PRA in preinduction 3T3-L1 cells

Mouse 3T3-L1 cells were treated with 0–20 μM RA and PRA at preinduction stage (Days −3 to 0), and cell cycle and apoptosis were determined by FACS analysis. Compared to RA treatment, an increased inhibition of apoptosis was observed with treatment with PRA at >10 μM (Fig. 3), although, up to 5 μM, the apoptosis rates of RA and PRA were similar. To confirm the results of FACS, BrdU incorporation analyses of 3T3-L1 preadipocytes between RA and PRA, by concentrations, were compared (data not shown). In DNA synthesis assay, cells were treated with RA and PRA for 3 days before incubation with BrdU. Although results were not significantly different up to 5 μM between RA and PRA treatments, similar to the results of FACS analysis, treatment with 10–20 μM PRA decreased apoptosis and increased DNA synthesis in 3T3-L1 preadipocytes, compared to RA treatment. On the other hand, PEG alone had no effect on apoptosis and DNA synthesis.

3.3. Reduction of differentiation and PPARγ2-induced adipogenesis in cultured 3T3-L1 preadipocytes by PRA

Long-term (15 days) treatment of 3T3-L1 preadipocytes with 1–10 μM RA and PRA was visualized by ORO

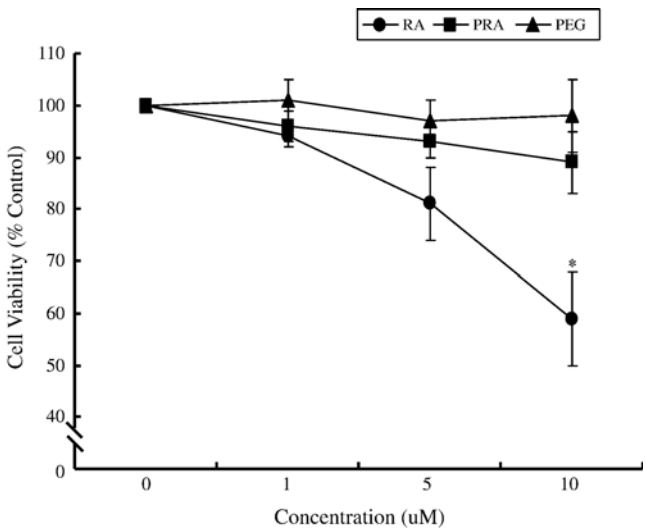

Fig. 6. Effect of 0–10 μM RA and PRA on the cell viability of cultured postinduction (Days 0–15) 3T3-L1 cells. Adipogenesis was induced by treatment with the cocktail of 3T3-L1 preadipocytes. Subsequently, the cells were treated with RA and PRA at indicated concentrations for 15 days. Postinduction 3T3-L1 preadipocytes were treated with cocktail for 15 days in the presence of 0–10 μM RA and PRA, respectively. Cell number was decreased by 10 μM RA treatment, whereas PRA did not affect cell viability with increasing concentrations in postinduction cells. Values are expressed as mean±S.D. *$P<.05$.

staining and was quantified as intracellular TG content. After 15 days of culture in the differentiation medium with cocktails, a high percentage of 3T3-L1 preadipocytes acquired the typical morphology of differentiated fat cells. At this time, lipid droplet was clearly detected by ORO staining of differentiated 3T3-L1 preadipocytes (Fig. 4A and B; control), which contained high levels of TG content (data not shown). By contrast, treatment with RA and PRA resulted in a marked reduction in lipid accumulation. GPDH activity was also completely down-regulated by RA and PRA treatments (Fig. 5A). We also checked whether treatment with RA and PRA for long time periods had an effect on PPARγ2 and C/EBPα expression in mature adipocytes (Fig. 5B). The results showed that PPARγ2 expression was significantly down-regulated after RA and PRA treatment during the entire differentiation period, compared to control cells, although the inhibition of adipocyte marker protein expression in 3T3-L1 preadipocytes in the presence of 10 μM RA was higher than that in the presence of 10 μM PRA. Moreover, no differences in PPARγ2 and C/EBPα expressions were observed between RA-treated and PRA-treated groups.

We further studied whether PRA regulated the expression of other PPARγ2 target genes such as *aP2*, whose products are important in the binding and transport of RA and PRA in adipose tissues. As shown in Fig. 5B, the expression pattern of aP2 was similar to that of PPARγ2, with the effect being most pronounced after treatment with RA and PRA. On the other hand, results of MTT assay showed that cell number markedly increased with PRA treatment, compared to RA treatment (Fig. 6), suggesting that, regardless of the medium used preinduction and postinduction, treatment of 3T3-L1 cells with 10 μM RA, compared with PRA treatment, resulted in a lower cell number, although cell numbers were

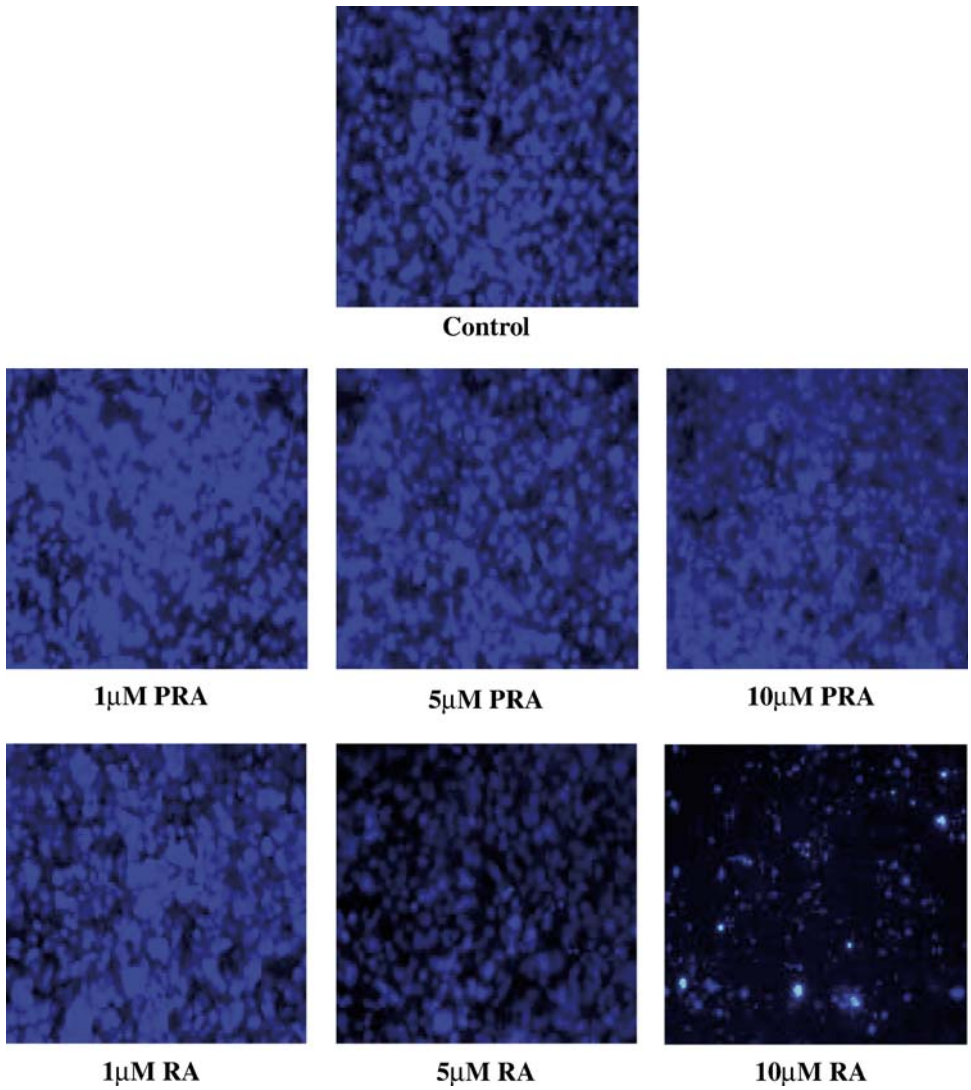

Fig. 7. Effect of 0–10 μM RA and PRA on DAPI staining of cultured postinduction (Days 0–15) 3T3-L1 cells. Adipogenesis was induced by treatment with the cocktail of 3T3-L1 preadipocytes. Subsequently, the cells were treated with RA and PRA at indicated concentrations for 15 days. Postinduction 3T3-L1 preadipocytes were treated with cocktail for 15 days in the presence of 0–10 RA and PRA, respectively. PRA did not affect apoptosis with increasing concentrations in postinduction cells, whereas apoptosis was increased by treatment with 10 μM RA.

not significantly different between RA and PRA up to 5 μM. To confirm the results of cell viability, DAPI stainings of 3T3-L1 preadipocytes between RA and PRA, by concentrations, were also compared (Fig. 7). The results showed that there was no significant difference in cell apoptosis rate between 0 and 5 μM RA and PRA, whereas 10 μM RA increased apoptosis compared to PRA treatment.

4. Discussion

Obesity is associated with a number of pathological disorders, such as non-INS-dependent diabetes, hypertension, hyperlipidemia and cardiovascular diseases [3], and is characterized by an increased adipose tissue mass that results from increases in both hyperplasia and hypertrophy [7]. Moreover, understanding of the balance between the positive and negative regulators of adipogenesis has important health-related implications for antiobesity medical therapy [32]. Some drugs are used for the therapy of obese-related metabolic diseases or in the discussion of the possibility of preventing body fat accumulation. However, the molecular basis for these associations remains to be elucidated, thus rendering the search for antiobesity agents inherently difficult. In this study, our interest was to determine how RA, which is known to have favorable effects on lipid homeostasis, affects lipid accumulation in adipocytes. Here, we found that PRA also inhibits the process of adipogenesis, including survival of adipocytes and differentiation to mature adipocytes, and may be developed to treat obesity.

Because RA is readily degraded upon exposure to light, oxidants and heat [33], the stability of RA is one important factor in drug formulation. Indeed, our study showed that RA dissolved in methanol rapidly degraded during incubation at room temperature under light exposure, whereas the rate of PRA degradation was very slow. On the other hand, when the samples were protected from light, no decreases in RA and PRA concentrations were observed (data not shown), suggesting that the rapid degradation of RA under our experimental settings was mainly caused by photolysis and that the conjugation of RA to PEG may be an effective means to protect RA from light. Generally, PEGylation increases the stability and safety of drugs [34]. In addition, PEGylated drugs are commercially available due to their amphiphilic nature and solubility in water and gained attention as enhancers of the absorption and bioavailability of certain drugs [34,35].

Many studies on adipose cell lines, including 3T3-L1, revealed that growth-arrested cells undergo at least one round of DNA replication and cell doubling before subsequent differentiation [36,37]. In our study, results of FACS analysis showed that RA-induced apoptosis with increasing concentrations in 3T3-L1 preadipocytes could be attributed to its effect on hyperplasia. In addition, the response of preinduction cells to RA treatment could be explained by a block at the G_0/G_1 phase, as judged by the appearance of a sub-G_1 peak during cell cycle progression, thereby reducing cell growth and inhibition of DNA synthesis. Support for these results comes from in vitro studies, demonstrating that a high concentration of RA induces apoptosis in preadipocytes [19].

Moreover, Suryawan and Hu [8] demonstrated that 25 μM RA achieved maximal inhibition of adipocyte differentiation. However, to avoid toxicity effect at >25 μM RA, they used 10 μM RA in subsequent experiments. On the contrary, PRA reduced apoptosis in 3T3-L1 cells compared to RA itself. Although the excellent stabilization of PRA in cell apoptosis needs to be further elucidated, one explanation for the observed stabilization may be that PEGylation provides stability and reduces cytotoxicity. Generally, when PEGylated drugs are compared to nonmodified drugs, PEGylation provides higher solubility in water and lower cytotoxicity to drugs [38]. In addition, PEGylation has been shown to be nontoxic and has been approved for use in humans [31]. Consequently, the nontoxic and nonimmunogenic properties of PEGylated drugs have been applied to reduce immunogenicity and to prolong circulation time in the blood [31,38,39]. Our results are in agreement with early studies indicating that PEGylation increases stability and reduces cytotoxicity in preinduction adipocytes.

Differentiation of adipocytes occurs in response to a variety of stimuli, including dietary constituents, drugs and nuclear hormone receptors [40]. In addition, INS is known to regulate adipocyte differentiation and lipid accumulation [41]. In our study, adipocyte precursor cells placed on cocktails such as INS, Dex and IBMX were able to undergo full maturation into adipocytes. It also expressed major adipocyte marker proteins such as PPARγ2, C/EBPα and aP2. The adipocyte differentiation program is regulated by the sequential expression of transcriptional activators, mainly PPAR families [42]. Especially, PPARγ2 is found almost exclusively in adipose tissues and has been linked to adipocyte differentiation [43]. Moreover, the γ subtype of PPAR is expressed at a high level in adipose tissues of mice, and its expression rapidly and dramatically increased during the differentiation of 3T3-L1 preadipocytes [44]. Furthermore, a combined expression of PPARγ and C/EBPα has synergistic effects on the promotion of fat cell conversion in myoblasts [45], showing that these genes are very important for adipocyte fat accumulation. By contrast, 5–10 μM RA significantly dedifferentiated adipocytes, as was similarly observed in PRA-inhibited lipid accumulation and differentiation in a dose-dependent and time-dependent manner. These results indicate that not only RA but also PRA has antioxidative action, thereby explaining the inhibition of 3T3-L1 cell differentiation, as similarly observed in RA-inhibited pig adipocyte differentiation [8] and RA inhibition of sheep adipocyte differentiation in primary culture [46]. In addition, these results indicate that the negative effect of PRA on adipogenesis was accompanied by the reduction of PPARγ2 protein in 3T3-L1 cells, which was accompanied by the attenuation of C/EBPα expression. Because PPARγ

is a key transcription factor in the induction of adipogenesis and lipid accumulation, PRA-induced down-regulation of PPARγ expression is likely to function similarly to the observed effects of RA on transcriptional metabolism. Similar results were observed by Schwarz et al. [47], who reported that RA does not prevent C/EBPβ induction but blocks the induction of PPARγ and C/EBPα, thereby reducing adipogenesis. In addition, it has been already reported that the inhibitory actions of adipocyte differentiation by RA are exhibited through RAR up-regulation and PPARγ2 suppression [48]. Based on these results, the ability of PRA to block PPARγ-induced adipocyte differentiation — in addition to its ability to block the transcriptional activity of C/EBPα — is expected to ligand endogenous RAR interfering with the function of PPARγ. In fact, retinoids regulate cellular functions by binding to intracellular RAR or RXR, and RA selectively binds to RAR, leading to the formation of an RAR–RXR heterodimer [8]. In addition, the nature of the cross-talk of RA actions between RARs, RXRs and PPARs via coactivators in adipose tissues will likely prove to be important for the process of adipogenesis [42]. Our data, together with these results, suggest that the inhibitory action of adipocyte differentiation by RA and PRA is exhibited through RAR up-regulation, and the suppression of PPARγ2 and PRA-induced antiadipogenic effect in 3T3-L1 cells could be attributed to its effect on adipose hypertrophy, which was accompanied by a strong inhibition of PPARγ2-induced transcriptional activity.

The predictive value of in vitro cytotoxicity test is based on the concept that toxic chemicals affect the basic functions of cells. Such functions are common to all cells; hence, toxicity can be measured by assessing cellular damages [49]. Interestingly, our results indicate a sensitivity difference between RA and PRA treatments. Our results showed that PRA-induced dedifferentiation effect in 3T3-L1 cells could be attributed to its effect on adipose hypertrophy, but not on hyperplasia. In addition, regardless of the medium used preinduction and postinduction, PRA treatment of 3T3-L1 preadipocytes resulted in a cell number higher than that in RA treatment, although cell numbers were not significantly different in preinduction and postinduction 3T3-L1 preadipocytes between 1 and 5 μM RA and PRA. The excellent stabilization of PRA in preinduction and postinduction adipocytes, although needing to be further elucidated, may be due to the stability and reduced cytotoxicity provided by PEGylation, as supported by in vitro and in vivo studies demonstrating that PEGylation provides better cell viability, decreases cytotoxicity [50], improves stability and reduces toxicity of drugs [34]. These results suggest that, regardless of the medium used preinduction and postinduction, PRA is a stable and valuable drug in that it has good stability and it reduces cytotoxicity by PEGylation.

In conclusion, we coupled PEG to RA to provide stability and to decrease cytotoxicity. PRA inhibition of adipogenesis was also examined to explore the molecular events that occur during the adipogenic differentiation process. We demonstrated that PRA inhibits the differentiation of 3T3-L1 preadipocytes and that the expression of major adipocyte marker proteins such as PPARγ2, C/EBPα and aP2 is also down-regulated by PRA in a time-dependent and dose-dependent manner. Apoptosis, in addition, increased as the concentration of RA increased, whereas PRA reduced apoptosis with increasing concentrations. Based on these results, PRA is more suitable and valuable as a drug in that it has good stability and it reduces cytotoxicity through PEGylation, although RA is also effective in the differentiation of adipocytes. Hence, PRA may prove to be a stable pharmaceutical drug for controlling the deposition of fats in the human body.

Acknowledgments

We thank the National Instrumentation Center for Environmental Management for providing DLS, FACS and ^{1}H NMR measurements. D.D. Guo and I.Y. Kim were recipients of BK 21 grant.

References

[1] Fruhbeck G, Gomez-Ambrosi J, Muruzabal FJ, Burrel MA. The adipocyte: a model for integration of endocrine and metabolic signaling in energy metabolism regulation. Am J Physiol Endocrinol Metab 2001;280:E827–47.
[2] Tang QQ, Jiang MS, Lane MD. Possible role of SpI as repressor of the C/EBPα gene in the adipocyte differentiation program. Mol Cell Biol 1999;19:4855–65.
[3] Alessi MC, Lijnen HR, Bastelica D, Irene JV. Adipose tissue and atherothrombosis. Pathophysiol Haemost Thromb 2004;33:290–7.
[4] Kelly DE, Goodpaster BH. Skeletal muscle triglyceride: an aspect of regional adiposity and insulin resistance. Diabetes Care 2001;24: 933–41.
[5] Lewis GF, Carpentier A, Adeli K, Giacca A. Disordered fat storage and mobilization in the pathogenesis of insulin resistance and type 2 diabetes. Endocr Rev 2002;23:201–9.
[6] Unger RH, Zhou YT. Lipotoxicity of beta-cells in obesity and in other causes of fatty acid spillover. Diabetes 2001;50:S118–21.
[7] Cho KJ, Moon HE, Moini H, Packer L, Yoon DY, Chung AS. α-Lipoic acid inhibits adipocyte differentiation by regulating pro-adipogenic transcription factors via mitogen-activated protein kinase pathways. J Biol Chem 2003;278:34823–33.
[8] Suryawan A, Hu CY. Effect of retinoic acid on differentiation of cultured pig preadipocytes. J Anim Sci 1997;75:112–27.
[9] Choi YD, Kim SY, Kim SH, Lee KS, Kim CH, Byun YR. Long-term delivery of all-*trans*-retinoic acid using biodegradable PLLA/PEG–PLLA blended microspheres. Int J Pharm 2001;215:67–81.
[10] Toma S, Isnardi L, Raffo P, Dastoli G, De Francisci E, Riccardt L, et al. Effects of all-*trans*-retinoic acid and 13-*cis*-retinoic acid on breast-cancer cell lines: growth inhibition and apoptosis induction. Int J Cancer 1997;70:619–27.
[11] Kalmekerian GP, Jasti RK, Celano P, Nelkin BD, Maarby M. All-*trans*-retinoic acid alters myc gene expression and inhibits in vitro progression in small-cell lung cancer. Cell Growth Differ 1994;5: 55–60.
[12] Giannini F, Maestro R, Vukosa T, Ijevic TV, Pomponi F, Boiocchi M. All-*trans*, 13-*cis* and 9-*cis* retinoic acids induce a fully reversible

growth inhibition in HNSCC cell lines: implications for in vivo retinoic acid use. Int J Cancer 1997;70:194–200.
[13] Ohyama M, Matsuda K, Torii S, Matsui T, Yano H, Kawada T, et al. The interaction between vitamin A and thiazolidinedione on bovine adipocyte differentiation in primary culture. J Anim Sci 1998;76:61–5.
[14] Gazit D, Ebner R, Kahn AJ, Derynck R. Modulation of expression and cell surface binding of members of the transforming growth factor beta superfamily during retinoic acid-induced osteoblastic differentiation of multipotential mesenchymal cells. Mol Endocrinol 1993;7:189–98.
[15] Leboy PS, Beresford JN, Devlin C, Owen ME. Dexamethasone induction of osteoblast mRNAs in rat marrow stromal cell cultures. J Cell Physiol 1991;146:370–8.
[16] Sklan D. Vitamin A in human nutrition. Prog Food Nutr Sci 1987;1:39–55.
[17] Snodgrass SR. Vitamin neurotoxicity. Mol Neurobiol 1992;1:41–73.
[18] Frankel SR, Eardley A, Lauwers G, Weiss M, Warrell RP. The "retinoic acid syndrome" in acute promyelocytic leukemia. Ann Intern Med 1992;117:292–6.
[19] Chawla A, Lazar M. Peroxisome proliferators and retinoid signaling pathways coregulate preadipocyte phenotype and survival. Proc Natl Acad Sci U S A 1994;91:1786.
[20] Delgado C, Francis GE, Fisher D. The uses and properties of PEG-linked proteins. Crit Rev Ther Drug Carrier Syst 1992;9:249–304.
[21] Allen TM. Long-circulating (sterically stabilized) liposomes for targeted drug delivery. Trends Pharmacol Sci 1994;15:215–20.
[22] Greenwald RB, Choe YH, Mcguire J, Conover CD. Effective drug delivery by PEGylated drug conjugates. Adv Drug Deliv Rev 2003;55:217–50.
[23] Tobio M, Sanchez A, Vila A, Soriano I, Evora C, Vila-Jato JL, et al. The role of PEG on the stability in digestive fluids and in vivo fate of PEG–PLA nanoparticles following oral administration. Colloids Surf B 2000;18:315–23.
[24] Fleming AB, Haverstick K, Saltzman WM. In vitro cytotoxicity and in vivo distribution after direct delivery of PEG–camptothecin conjugated to the rat brain. Bioconjug Chem 2004;15:1364–75.
[25] Scott MD, Chen AM. Au-dela du GR: traitement par PEG des cellules sanguines et autres tissue [Beyond the red cell: pegylation of other blood cells and tissues]. Transfus Clin Biol 2004;11:40–6.
[26] Wise LS, Green H. Participation of one isozyme of cytosolic glycerophosphate in adipose conversion of 3T3 cells. J Biol Chem 1979;254:273–5.
[27] Bradford MM. A rapid and sensitive method for the quantitation of microgram quantities of protein utilizing the principle of protein dye binding. Anal Biochem 1976;72:248–54.
[28] Suryawan A, Hu CY. Effect of serum on differentiation of porcine adipose stromal–vascular cells in primary culture. Comp Biochem Physiol 1993;105A:485–92.
[29] Moghimi SM, Hunter AC, Murray JC. Nanomedicine: current status and future prospects. FASEB J 2005;19:311–30.
[30] Kim K, Luu YK, Chang C, Fang D, Hsiao BS, Chu B, et al. Incorporation and controlled release of a hydrophilic antibiotic using poly(lactide–co-glycolide)-based electrospun nanofibrous scaffolds. J Control Release 2004;98:47–56.
[31] Harris JM. Poly(ethylene glycol) chemistry: biotechnical and biomedical applications. New York: Plenum; 1992.
[32] Harp JB. New insights into inhibitors of adipogenesis. Curr Opin Lipidol 2004;15:303–7.
[33] Brisaert M, Gabriels M, Plaizier-Vercammen J. Investigation of the chemical stability of an erythromycin–tretionin lotion by the use of an optimization system. Int J Pharm 2000;197:153–60.
[34] Claudia FP. Safety assessment on poly(ethylene glycols) (PEGs) and their derivatives as used in cosmetic products. Toxicology 2005;214:1–38.
[35] Mu L, Feng SS. PLGA/TPGS nanoparticles for controlled release of paclitaxel; effects of the emulsifier and drug loading ratio. Pharm Res 2003;20:1864–72.
[36] Cao Z, Umek RM, Mcknight SL. Regulated expression of three C/EBP isomers during adipose conversion of 3T3-L1 cells. Genes Dev 1991;5:1538–52.
[37] Shao D, Lazar MA. Peroxisome proliferators activated receptor γ, CCAAT/enhancer binding protein α, and cell cycle status regulate the commitment to adipocyte differentiation. J Biol Chem 1997;272:21473–8.
[38] Kichler A. Gene transfer with modified polyethylenimines. J Gene Med 2004;6:S3–S10.
[39] Kwon GS, Kataoka K. Block copolymer micelles as long circulating drug vehicles. Adv Drug Deliv Rev 1995;16:295–309.
[40] Burris TP, Pelton PD, Zhou L, Osborne MC, Cryan E, Demarest KT. A novel method for analysis of nuclear receptor function at natural promoters: peroxisome proliferators-activated receptor gamma agonist actions aP2 gene expression detected using branched DNA messenger RNA quantitation. Mol Endocrinol 1999;13:410–7.
[41] Scavo LM, Karas M, Murray M, Leroith D. Insulin-like growth factor-I stimulates both cell growth and lipogenesis during differentiation of human mesenchymal stem cell into adipocytes. J Clin Endocrinol 2004;89:3543–53.
[42] Kawada T, Kamei Y, Fujita A, Hida Y, Takahashi N, Sugimoto E, et al. Carotenoids and retinoids as suppressors on adipocyte differentiation via nuclear receptors. Biofactors 2000;13:103–9.
[43] Tontonoz P, Hu E, Spiegelman BM. Regulation of adipocyte gene expression and differentiation by peroxisome proliferators-activated receptor gamma. Curr Opin Genet Dev 1995;5:571–6.
[44] Gearing KL, Gottlicher M, Widmark E, Banner CD, Tollet P, Stromstedt M, et al. Fatty acid activation of the peroxisome proliferators activated receptor, a member of the nuclear receptor gene superfamily. J Nutr 1994;124:1284–8.
[45] Dalei S, Lazar MA. Peroxisome proliferators activated receptor γ, CCAAT/enhancer-binding protein α, and cell cycle status regulate the commitment to adipocyte differentiation. 1997;272:21473–8.
[46] Torii S, Matsumoto K, Maysui T, Yano H. Effect of vitamin A, C and D on glycerol-3-phosphate dehydrogenase activity of sheep preadipocytes in primary culture. Anim Sci Technol 1995;66:1039–42.
[47] Schwarz EJ, Reginato MJ, Shao D, Krakow SL, Lazar MA. Retinoic acid blocks adipogenesis by inhibiting C/EBPbeta-mediated transcription. Mol Cell Biol 1997;17:1552–61.
[48] Brebourg TD, Hu CY. Regulation of differentiating pig preadipocytes by retinoic acid. J Anim Sci 2005;83:98–107.
[49] Shirui M, Xintao S, Florian U, Mittmar W, Xiulan X, et al. Synthesis, characterization and cytotoxicity of poly(ethylene glycol)–graft–trimethyl chitosan block copolymer. Biomaterials 2005;26:6343–56.
[50] Li C, Yu D, Inoue T, Yang DJ, Milas L, Hunter NR, et al. Synthesis and evaluation of water-soluble polyethylene glycol–paclitaxel conjugate as a paclitaxel prodrug. Anticancer Drugs 1996;7:642–8.